RE-2022-269188 - Turnitin Plagiarism Report

by Roshan Samuel J

Submission date: 13-May-2024 08:22AM (UTC+0100)
Submission ID: 271715604863
File name: RE-2022-269188.docx (3.29M)
Word count: 2923
Character count: 18053

Mammogram Cancer Detection and Classification

1. Abstract

Breast cancer remains a significant health concern globally, emphasizing the need for advanced technologies to improve detection and classification. This paper presents a deep learning approach aimed at enhancing breast cancer detection and classification accuracy. Mammogram Cancer Detection has leveraged their ability to learn complex patterns from medical imaging data. The first phase of the system involves pre-processing mammography images to enhance quality and normalize variations. Subsequently, a CNN architecture is employed for automatic feature extraction, capturing intricate details relevant to breast cancer diagnosis. Transfer learning techniques are integrated to leverage pre-trained models and optimize performance, especially with limited training data.

Keywords: Mammogram

2. Introduction

The human body's intricacies are epitomized in the functionality of the breasts, pivotal not only in nurturing infants but also in reflecting health conditions, notably concerning breast cancer. Breast cancer stands as a formidable adversary, arising from abnormal cell growth within breast tissues, and is a leading cause of cancer-related mortality among women worldwide [1] [. Hormonal factors, particularly prolonged exposure to estrogen and progesterone, can also contribute to tumor growth, as seen in hormone receptor-positive breast cancers Environmental factors like radiation exposure, certain chemicals, and lifestyle habits such as alcohol consumption and smoking further accentuate the risk profile. Despite progress in screening and diagnostic capabilities, challenges persist in achieving accurate and timely detection of breast cancer, especially in subpopulations with unique risk profiles or limited access to healthcare resources. Addressing these challenges requires a multifaceted approach encompassing technological innovation, healthcare infrastructure development, risk assessment strategies, and patient education and empowerment. In this report, we delve into the landscape of breast cancer detection, exploring the complexities of risk factors, diagnostic methodologies, technological innovations, and challenges in current practices. Through a comprehensive analysis, we aim to elucidate the current state of breast cancer detection, identify areas for improvement

3. Related Works

The domain of breast cancer detection were prominent and these methods often focused on feature extraction using techniques such as wavelet transforms, texture analysis, and morphological operations. For instance, researchers in utilized Gaussian filtering and probabilistic neural networks for accurate tumor detection, achieving a commendable accuracy of 98%. Similarly, authors in [9] developed a model incorporating morphological operations, median filtering, and support vector machines (SVMs), boasting a remarkable 99% accuracy in classifying malignant tumors. The evolution towards deep learning models brought about a paradigm shift in breast cancer detection. For instance, researchers in [13] employed transfer learning with a pre-trained GoogLeNet model, achieving a mean classification accuracy of 98% on brain MRI images. The comparative analysis of deep learning models in breast cancer detection has been a focus of several studies [11, 16]. Researchers in [11] compared the performance of AlexNet, VGG Net, and GoogLeNet, finding that VGG-16 outperformed others with an accuracy of up to 98.69%. Similarly, authors in [16] utilized the ResNet-50 model for brain cancer diagnosis, achieving a classification accuracy of 97.2%. Hybrid models combining deep learning and traditional machine learning techniques have also garnered attention [24, 25]. These hybrid approaches leverage the strengths of both methodologies, enhancing efficiency and accuracy in tumor detection and classification. Furthermore, studies focusing on multimodal medical image fusion [26] and novel feature extraction techniques [27] have contributed to the advancement of breast cancer detection systems. Overall, the Mammogram Cancer Detection gives a effcient to overcome it and save the women's sufferings……

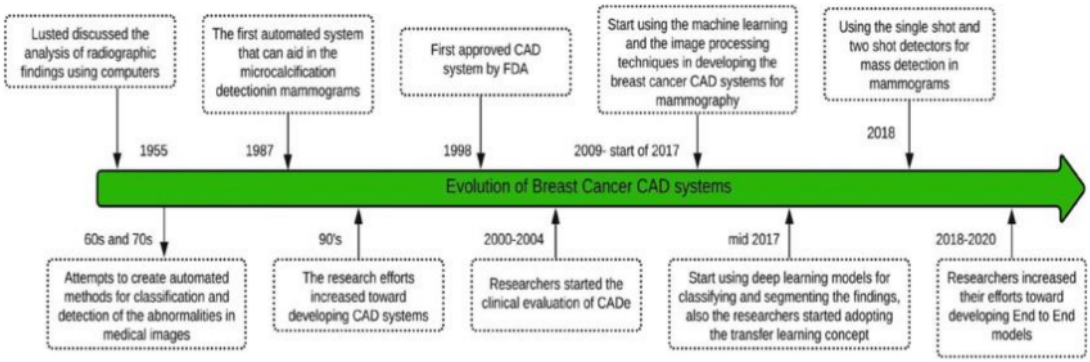

Figure 1: Mammogram cancer detection timelines

3. Proposed Work

Mammogram Acquisition: Obtain mammogram images from medical imaging sources.
Contrast Enhancement: Enhance the contrast of mammogram images to improve visibility and feature detection.
Pectoral Muscle Removal: Use image processing techniques to remove the pectoral muscle area from mammogram images, focusing on the breast tissue region of interest.
SOM Clustering: Apply Self-Organizing Map (SOM) clustering to segment and group regions of interest within the mammogram images, potentially identifying abnormal areas indicative of tumors or lesions.
ROM Extraction: Extract Region of Interest (ROM) features from the clustered mammogram images, capturing specific characteristics relevant to breast abnormalities.
Curvelet Transform: Utilize the curvelet transform for multi-scale analysis of mammogram images, enhancing the representation of features at different frequencies and orientations.
Scale 1 Sparse Coefficient to N Sparse Coefficient: Transform the mammogram images into a sparse representation, focusing on relevant coefficients at different scales to reduce noise and extract essential information.
Sparse Curvelet Coefficient: Further process the sparse coefficients obtained from the curvelet transform, emphasizing key features while minimizing redundant information.
LBP Pattern: Apply Local Binary Patterns (LBP) to extract texture features from the mammogram images, capturing patterns and structures that may indicate abnormalities.
ANN Classification: Employ Artificial Neural Networks (ANNs) for classification tasks, training the network on extracted features from mammogram images to differentiate between normal and abnormal breast tissues.

Proposed Methodology:

Pre-process mammogram images to ensure uniformity and quality.
Apply contrast enhancement techniques to improve image clarity.
Remove the pectoral muscle region to focus on breast tissue.
Use SOM clustering to identify potential abnormal areas.
Extract ROM features from clustered regions for detailed analysis.
Apply curve-let transform and sparse coefficient representations for feature extraction.
Utilize LBP patterns for texture analysis and feature enhancement.
Train an ANN classifier using the extracted features to classify mammogram images as normal or abnormal (potentially indicating the presence of tumors or lesions).

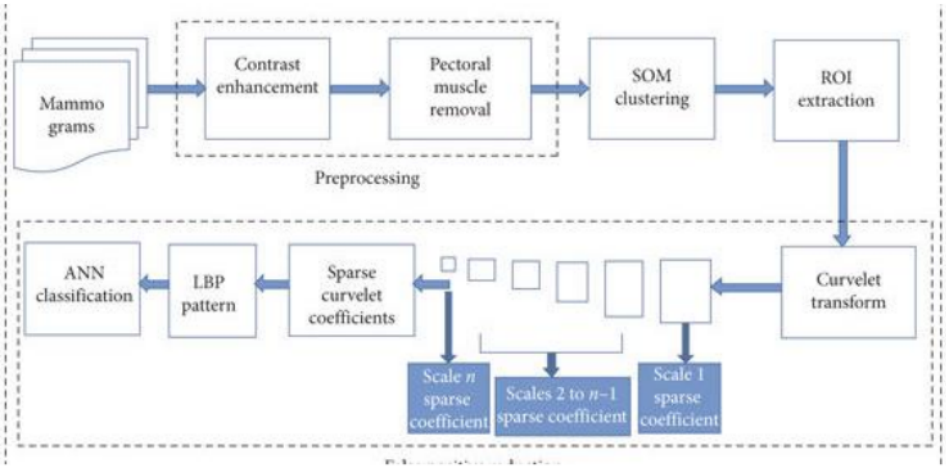

Figure 2: Mammogram Cancer Detection Architecture

3.1 First Phase: Image Preprocessing

Image pre-processing in mammogram cancer detection is a crucial step aimed at improving the quality of input images to facilitate more accurate analysis. This process involves several techniques designed to standardize, enhance, and isolate relevant regions within the images. Firstly, resizing and rescaling are employed to ensure uniformity in image dimensions, aiding in consistent analysis across datasets. Normalization further refines the images by scaling pixel values to a common range, typically between 0 and 1, which helps in achieving better model convergence during subsequent analysis steps. Noise reduction techniques such as Gaussian blur or median filtering are applied to reduce unwanted artifacts and improve image clarity, essential for precise feature extraction. which involves identifying and isolating relevant regions such as the breast area from the background, ensuring focused analysis on specific anatomical structures critical for accurate breast cancer detection algorithms. Collectively, these pre-processing techniques lay the foundation for robust and reliable image analysis, contributing significantly to the effectiveness of mammogram cancer screening.

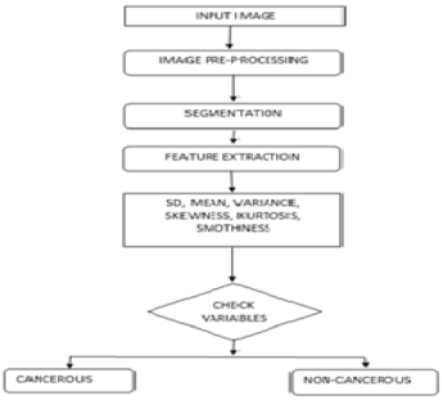

Figure 3: Block diagram of Mammogram Cancerous Detection

3.2 Second Phase

Segmentation is a pivotal stage in breast cancer detection, focusing on dividing the image into meaningful regions or objects to isolate specific areas of interest, such as

breast tissue, from the surrounding background or other structures. Several techniques are employed in segmentation to achieve this purpose effectively. Thresholding is a fundamental technique that partitions the image based on pixel intensity thresholds, enabling the separation of foreground elements like breast tissue from the background. Edge detection techniques, such as Canny edge detection or Sobel operators, play a crucial role in identifying edges or boundaries within the image, which helps delineate structures and boundaries of interest. Additionally, region growing methods are utilized to group pixels with similar properties, forming distinct regions that aid in segmenting and outlining structures within the image, contributing significantly to the accurate characterization and analysis of breast tissue in the context of cancer detection algorithms. Integrating these segmentation techniques enables the creation of precise and detailed regions of interest essential for subsequent feature extraction and classification stages in breast cancer detection systems.

Third Phase : Feature Extraction

Statistical Features: Statistical descriptors such as Standard Deviation (SD), Mean, Variance, Skewness, Kurtosis, and Smoothness are computed within segmented regions. These features capture the distribution and variation of pixel intensities, providing valuable information about the texture and structure of the tissue. For instance, malignant tissues may exhibit high variability (e.g., higher SD and kurtosis) compared to benign tissues.

Texture Features: Texture patterns are captured using methods like Gray Level Co-occurrence Matrix (GLCM), which calculates texture properties such as homogeneity, contrast, energy, and correlation within segmented regions. Texture features are crucial in distinguishing between different tissue types based on their microstructural properties. Malignant tissues often exhibit irregular and heterogeneous textures compared to the more uniform textures of benign tissues.

Shape Features: Shape characteristics such as area, perimeter, circularity, and compactness are extracted to describe the shape of detected regions. These features provide insights into the geometric properties of the tissue and can be indicative of malignancy. For example, malignant tumors may have irregular shapes and higher irregularity (e.g., lower circularity) compared to benign

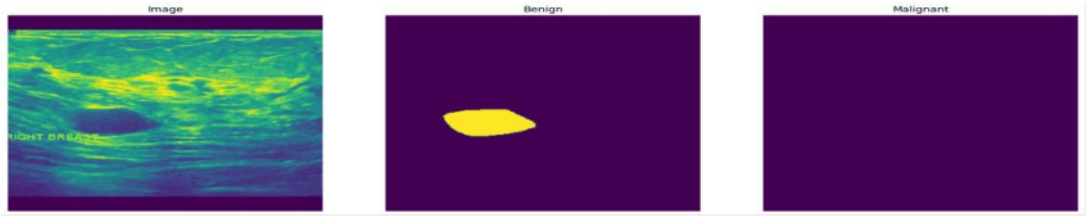

Figure 5: Mammogram Cancer Detection (a) Benign (b) Malignant

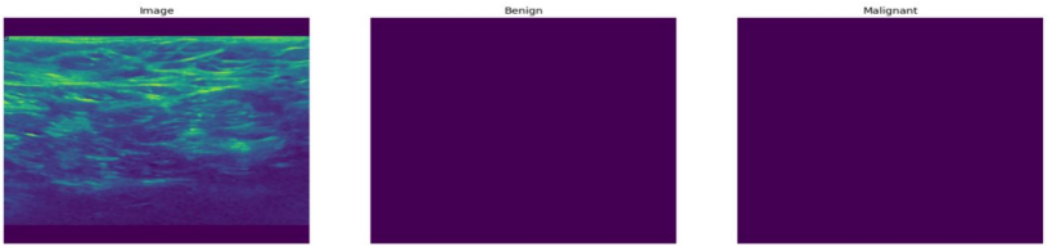

Figure 6: Mammogram Cancer Detection (a) Benign (b) Malignant

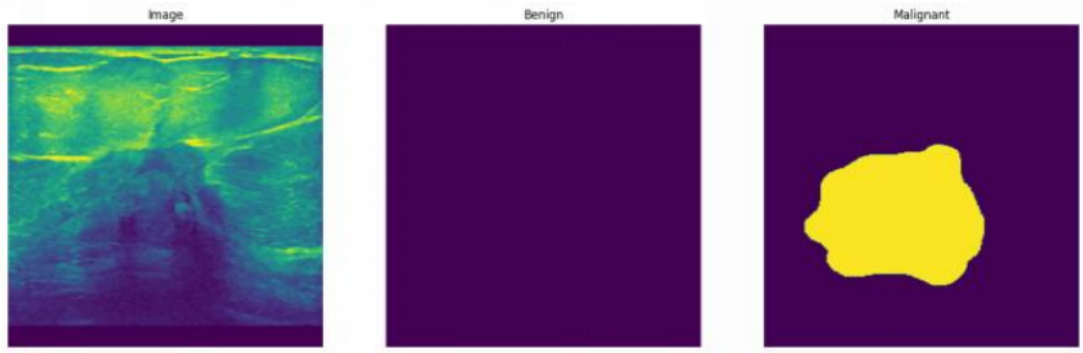

Figure 7: Example 3 of Mammogram Cancer Detection (a) Benign (b) Malignant

3.3 Mammogram Cancer Classification Phases

Classification

In the classification stage of breast cancer detection, the primary goal is to categorize segmented regions or extracted features as either cancerous or non-cancerous based on learned patterns. This process involves utilizing various techniques:

Networks are trained using extracted features as input to predict whether a region is cancerous or non-cancerous. These algorithms learn patterns from the data and can generalize well to new, unseen cases, contributing to accurate classification.

Deep Learning: Deep learning techniques, especially (CNNs), are utilized to learn complex patterns directly from images. CNNs can automatically extract hierarchical features from images, making them particularly effective for image classification tasks such as distinguishing between cancerous and non-cancerous regions based on the learned representations.

Feature Selection: Feature selection techniques, such as Principal Component Analysis (PCA) or feature importance ranking, are employed to choose the most informative features that contribute significantly to classification accuracy. By selecting relevant features and reducing dimensionality, feature selection methods enhance the efficiency and performance of classification.

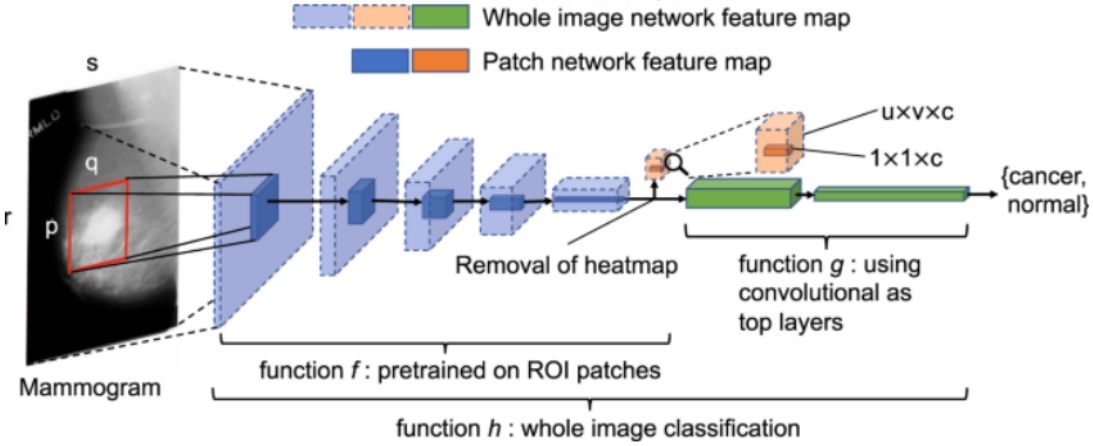

Figure 9: Architecture of the Detection of screening Mammography

- **Convolutional Layer**

"The Inception V3 model utilized in the Auto Contrast Enhancer, Tumor Detector, and Classifier comprises 94 convolution layers. Each convolution layer takes the input image as a matrix, performs the convolution operation, and generates feature maps of the input image. The convolution operation is a linear process depicted in Equation (1), where 'w'

and 'x' represent the inputs from the previous layer, 'm x n' signifies the size of the CNN matrix, and 'y' denotes the output of the CNN layer. The initial convolution layer is equipped with a kernel of dimensions 11 x 11 x 3. Subsequently, the remaining 93 convolution layers employ kernels sized at 5 x 5 x 48 [reference 29]."

$$y(i,j) = x(i,j) * w(i,j) = \sum_m \sum_m x(m,n)\, w(i-m, j-n) \quad (1)$$

- **Activation Function**

"In multilayer artificial neural networks or deep neural networks, activation functions such as Sigmoid, Tanh, and ReLU [16] play a crucial role in applying nonlinear transformations to the outputs from convolution operations. In the proposed model, the authors opted for the ReLU activation function, described in Equation (2). This choice addresses the vanishing gradient problem commonly encountered in deep neural networks, where weights diminish to extremely small values, impeding model convergence and optimal solution attainment."

$$Relu: f(y) = \begin{cases} 0, & y < 0 \\ 1, & y \geq 0 \end{cases} \quad (2)$$

- **Batch Normalization**

"Batch normalization plays a crucial role in normalizing the outputs from convolutions, aiding in the rapid training of the network and mitigating covariance shift [17]. The definition of batch normalization is presented in Equation (3), where 'M' represents the number of input data items, denotes the average value of the stack, signifies the normalized values obtained from the process, and stands for the standard deviation of the stack."

$$Y_i = \frac{X_i - \mu_\beta}{\sqrt{\sigma_\beta^2 + \epsilon}} \quad (3)$$

Here, $\sigma_\beta = \frac{1}{M}\sum_{i=1}^{M}(X_i - \mu_\beta)^2$ and $\mu_\beta = \frac{1}{M}\sum_{i=1}^{M} X_i$; i =1, 2….M

- **Pooling Layer**

"The convolutional layer simplifies the information from the input by creating a summary feature map based on the feature maps produced earlier. In deep convolutional neural networks, max-pooling and average-pooling are common pooling layers [3]. In the proposed model, the authors included a max-pooling layer with a filter size of N×N, where N is three.

Equation (4) is used to determine the dimensions of the output image after pooling, where:

'H' is the height,
'W' is the width,
'D' is the depth of the input image,
'F' is the filter size,
'S' is the number of steps used,
'R' is the size of the resultant image.
The Flattening Layer converts the multidimensional outputs from the previous layer into a one-dimensional array to connect with neurons in the next layer.

The Dropout Layer prevents overfitting by randomly dropping connections during training, specified by a dropout probability (e.g., 20%). This simplifies implementation compared to training multiple models for ensemble techniques. In this research, a dropout of 0.2 was used.

The Fully Connected (FC) layer groups input into distinct categories based on features extracted earlier. Equation (5) defines the fully connected layer in a feed-forward network."

$$y_i^n = f(u_i^n) + b^{(n)} \quad (6)$$

"Here, 'w_ji^(n-1)' represents the weight of neurons in the hidden layer, 'y_j^(n-1)' is the value of input neurons, 'u_i^n' denotes the value of the resultant layer before the activation function, and 'b^((n))' is the bias value. 'n' represents the total number of layers, 'i' and 'j' denote the number of neurons, and 'y_i^n' represents the value in the resultant layer."

4. Analysis and Results of Mammogram Cancer Detection

4.1 Dataset that is used

"In order to evaluate the effectiveness of the suggested strategy, the authors of this work employed the publicly accessible Fig sharing database [15]. This collection, created by Arya Shah in 2021, includes 397 breast MRI photos from 233 different individuals as the testing dataset and 3,064 breast MRI photographs as the training dataset. Additionally, the database includes MRI images of individuals with benign and/or malignant breast tumors.

The training dataset consists of 891 MRI images of benign tumors and 2,284 MRI images of malignant

tumors. On the other hand, the testing dataset includes 421 MRI images of benign tumors and 178 MRI images of malignant tumors. In total, there are 891 benign tumor images, 2,284 malignant tumor images, and 266 normal images in the dataset. Figure 10 displays samples of MRI images used for testing in this study."

Table 1: Information on the testing and training datasets that are used to classify and identify tumours

.

Images Count	Trained Dataset		Tested Dataset	
	Benign	Malignant	Benign	Malignant
1,578	891	421	440	211

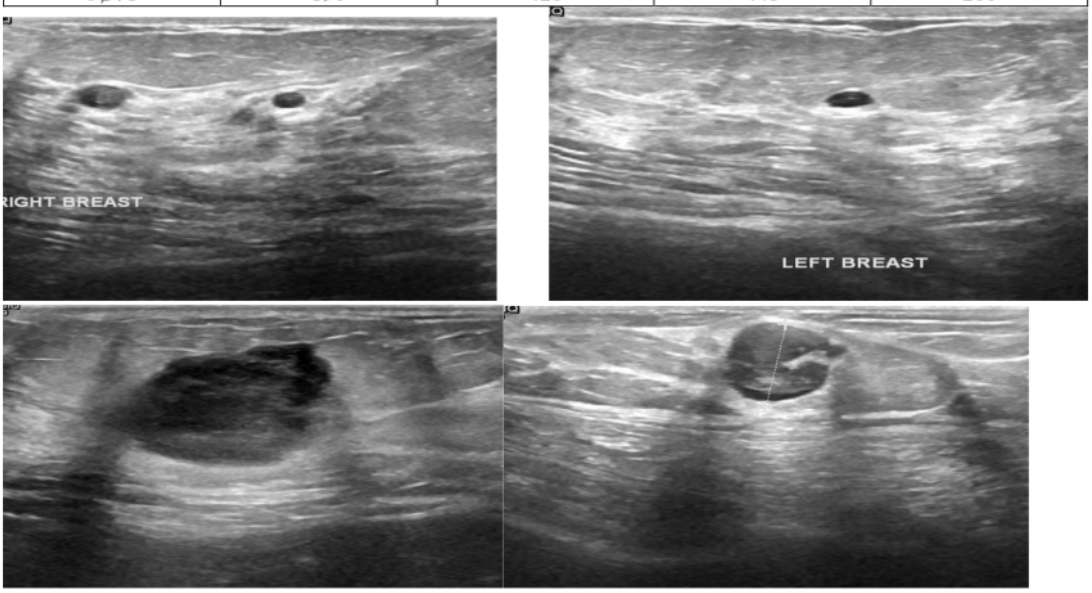

Figure 10: Benign and Malignant Cancer Top and Bottom View

4.2 Model Comparison and Analysis

Among the listed architectures and their respective accuracy values, Efficientb1 (EfficientNet B1) stands out with a remarkable accuracy of 100%. EfficientNet B1 is well known for making it a popular choice for various computer vision tasks. Other architectures in the comparison include Densenet, InceptionV3, MobileNet, MobileNetv2, resnet18, resnet34, resnet50, and Efficientnetb0 (EfficientNet B0), each with their own accuracy scores ranging from 12.5% to 100%.

Architecture	Accuracy
Densenet	0.49965
Efficientb1	1.00000
InceptionV3	0.12500
MobileNet	0.80000
MobileNetv2	0.75000
resnet18	0.62500
resnet34	0.50000
resnet50	0.66667
Efficientnetb0	0.50076

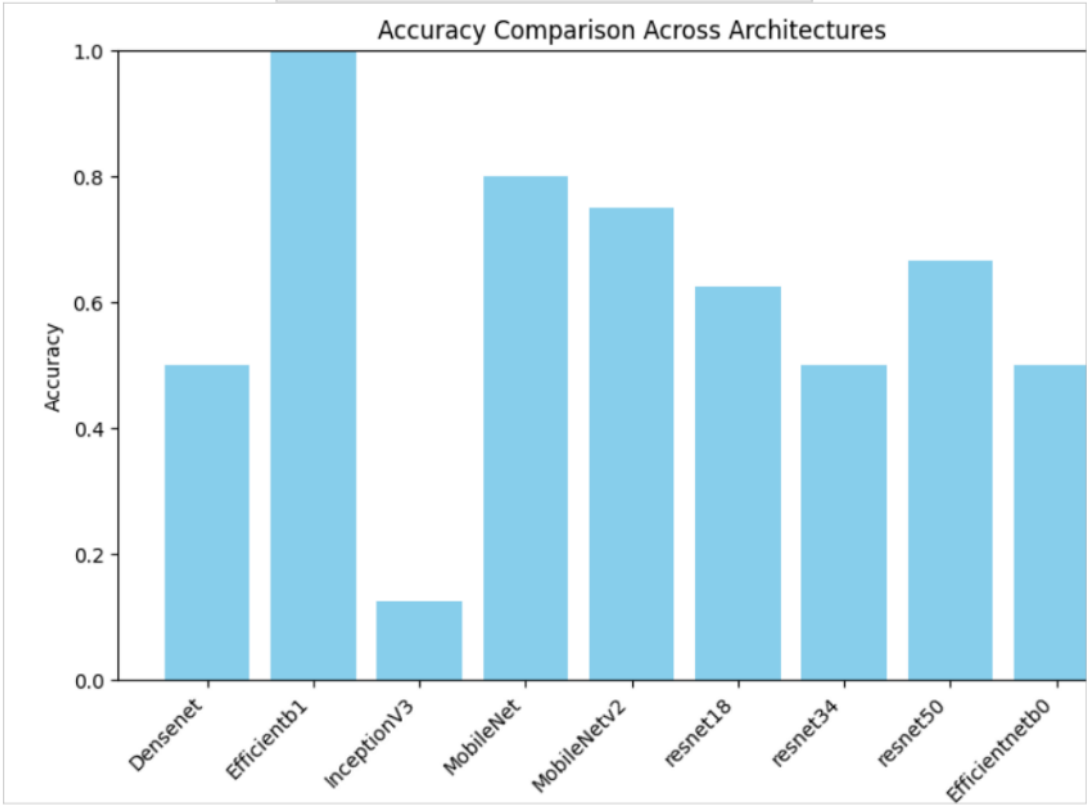

MATHEMATICAL EQUATIONS OF THE MODELS

ResNet18 and ResNet34:

$$\text{Output} = \text{ReLU}(F_2(\text{ReLU}(F_1(\text{Input}))) + \text{Input})$$

Resnet50:

$$\text{Output} = \text{ReLU}(F_3(F_2(F_1(\text{Input}))) + \text{Input})$$

$$\text{Output} = \text{PointwiseConv}(\text{ReLU}(\text{DepthwiseConv}(x, k_1)), k_2) + x$$

Where:

- x is the input feature map.
- k_1 and k_2 are the depth-wise and point-wise convolution kernels, respectively.
- DepthwiseConv represents depth-wise convolution.
- PointwiseConv represents point-wise convolution.
- ReLU is the Rectified Linear Unit activation function.

MobileNetV2:

$$\text{Output} = x + \text{PointwiseConv}(\text{ReLU}(\text{DepthwiseConv}(\text{PointwiseConv}(x, k_1), k_2)), k_3)$$

Where:

- x is the input feature map.
- k_1, k_2, and k_3 are the point-wise convolution kernels.
- $\mathrm{DepthwiseConv}$ represents depth-wise convolution.
- $\mathrm{PointwiseConv}$ represents point-wise convolution.
- ReLU is the Rectified Linear Unit activation function.

These expressions capture the fundamental operations of MobileNet and MobileNetV2, with MobileNetV2 introducing the inverted residual block to enhance performance and efficiency.

MobileNetv1:

1. **Normal Cell Operation**:

$$\mathrm{NormalCell}(x) = \mathrm{Concatenate}(\mathrm{Operation}_1(x), \mathrm{Operation}_2(x)) + \mathrm{SkipConnection}(x)$$

2. **Reduction Cell Operation**:

$$\mathrm{ReductionCell}(x) = \mathrm{Concatenate}(\mathrm{Operation}_1(x), \mathrm{Operation}_2(x)) + \mathrm{SkipConnection}($$

Custom CNN:

$$\text{Output} = \text{Softmax}(\text{Dense}(\text{Flatten}(\text{MaxPooling2D}(\text{ReLU}(\text{Conv2D}(\text{Input})))))))$$

Where:

- Input represents the input image tensor.
- ReLU represents the rectified linear unit activation function.
- MaxPooling2D represents the max pooling operation.
- Conv2D represents the 2D convolution operation.
- Flatten represents the flattening operation.
- Dense represents the fully connected layer.
- Softmax represents the softmax activation function.

Resnet101:

Let $X^{(l)}$ denote the output tensor of layer l, $W^{(l)}$ denote the weight tensor, $b^{(l)}$ denote the bias vector, and σ denote the activation function.

$$X^{(l)} = \begin{cases} \sigma\left(\sum_{m=0}^{K^{(l)}-1}\sum_{n=0}^{K^{(l)}-1}\sum_{p=0}^{C^{(l-1)}-1} W_{m,n,p,k}^{(l)} X_{i\times S^{(l)}+m, j\times S^{(l)}+n, p}^{(l-1)} + b_k^{(l)}\right) & \text{if } l \text{ is a convolutional la} \\ \max_{m,n}\left(X_{i\times S^{(l)}+m, j\times S^{(l)}+n, k}^{(l-1)}\right) & \text{if } l \text{ is a max-pooling lay} \\ \sigma(W^{(l)} X^{(l-1)} + b^{(l)}) & \text{if } l \text{ is a fully connected} \end{cases}$$

InceptionV3:

Let $X^{(l-1)}$ denote the input tensor to the l-th layer.

The output of the l-th layer, $X^{(l)}$, can be expressed as:

$$X^{(l)} = \text{Concatenate}\left(X_{1x1}^{(l)}, X_{3x3}^{(l)}, X_{5x5}^{(l)}, X_{\text{pool}}^{(l)}, X_{\text{factorized}}^{(l)}, X_{\text{avg\_pool}}^{(l)}, X_{\text{fc}}^{(l)}\right)$$

Where:

- $X_{1x1}^{(l)}$, $X_{3x3}^{(l)}$, $X_{5x5}^{(l)}$, and $X_{\text{pool}}^{(l)}$ represent the outputs of the 1×1 convolution, 3×3 convolution, 5×5 convolution, and max pooling branches, respectively, within the Inception module.
- $X_{\text{factorized}}^{(l)}$ represents the output of the factorized convolution operation.
- $X_{\text{avg\_pool}}^{(l)}$ represents the output of the global average pooling operation.
- $X_{\text{fc}}^{(l)}$ represents the output of the fully connected layers.

Inception V1:

Let $X^{(l-1)}$ denote the input tensor to the l-th layer.

The output of the l-th layer, $X^{(l)}$, can be expressed as:

$$X^{(l)} = \text{Concatenate}\left(X_{1x1}^{(l)}, X_{3x3\_reduce}^{(l)}, X_{3x3}^{(l)}, X_{5x5\_reduce}^{(l)}, X_{5x5}^{(l)}, X_{\text{pool}}^{(l)}, X_{\text{factorized}}^{(l)}, X_{\text{avg\_pool}}^{(l)}, X_{\text{fc}}^{(l)}\right)$$

Where:

- $X_{1x1}^{(l)}$, $X_{3x3\_reduce}^{(l)}$, $X_{3x3}^{(l)}$, $X_{5x5\_reduce}^{(l)}$, and $X_{5x5}^{(l)}$ represent the outputs of different branches within the Inception module.
- $X_{\text{pool}}^{(l)}$ represents the output of the max pooling branch.
- $X_{\text{factorized}}^{(l)}$ represents the output of the factorized convolution operation.
- $X_{\text{avg\_pool}}^{(l)}$ represents the output of the global average pooling operation.
- $X_{\text{fc}}^{(l)}$ represents the output of the fully connected layers.

InceptionV2:

Let $X^{(l-1)}$ denote the input tensor to the l-th layer.

The output of the l-th layer, $X^{(l)}$, can be expressed as:

$$X^{(l)} = X_{\text{residual}}^{(l)} + X_{\text{concat}}^{(l)}$$

Where:

- $X_{\text{residual}}^{(l)} = X^{(l)} + X^{(l-1)}$ represents the residual connection between the output and input of the Inception module.
- $X_{\text{concat}}^{(l)}$ represents the concatenated output of the Inception module's branches, including 1×1, 3×3, 5×5 convolutions, pooling, factorized convolutions, global average pooling, and fully connected layers.

EfficientNet

Let $X^{(l-1)}$ denote the input tensor to the l-th layer.

The output of the l-th layer, $X^{(l)}$, can be expressed as:

$$X^{(l)} = \sigma\left(W^{(l)} * X^{(l-1)} + b^{(l)}\right)$$

Where:

- $*$ denotes the convolution operation.
- σ denotes the activation function (e.g., ReLU).
- $W^{(l)}$ denotes the weights of the convolutional filter.
- $b^{(l)}$ denotes the bias term.

Let $X^{(l-1)}$ denote the input tensor to the l-th layer.

The output of the l-th layer, $X^{(l)}$, can be expressed as:

$$X^{(l)} = \sigma\left(W^{(l)} * X^{(l-1)} + b^{(l)}\right)$$

Where:

- $*$ denotes the convolution operation.
- σ denotes the activation function (e.g., ReLU).
- $W^{(l)}$ denotes the weights of the convolutional filter.
- $b^{(l)}$ denotes the bias term.

Let $X^{(l-1)}$ denote the input tensor to the l-th layer.

The output of the l-th layer, $X^{(l)}$, within a dense block, can be expressed as:

$$X^{(l)} = H^{(l)}\left([X^{(0)}, X^{(1)}, \ldots, X^{(l-1)}]\right)$$

Where:

- $H^{(l)}$ represents the composite function of the l-th layer, typically consisting of batch normalization, activation, and convolutional operations.
- $[X^{(0)}, X^{(1)}, \ldots, X^{(l-1)}]$ denotes the concatenation of feature maps from all preceding layers within the same dense block.

The output of the l-th transition layer, denoted as $Y^{(l)}$, can be expressed as:

$$Y^{(l)} = \text{BatchNorm}\left(\text{ReLU}\left(W^{(l)} * X^{(l)} + b^{(l)}\right)\right)$$

Where:

- $W^{(l)}$ denotes the weights of the convolutional filter.
- $b^{(l)}$ denotes the bias term.
- $*$ denotes the convolution operation.

At the end of the network, the output Z can be expressed as:

$$Z = \text{Softmax}\left(W_{\text{fc}} \cdot \text{GlobalAvgPool}\left(Y^{(L)}\right) + b_{\text{fc}}\right)$$

Xception:

1. Depthwise seperable convolutions:

$$X^{(l)} = \text{PointwiseConv}\left(\text{DepthwiseConv}\left(X^{(l-1)}\right)\right)$$

2. Residual Connections:

$$X^{(l)} = X^{(l)} + F\left(X^{(l-1)}\right)$$

where F represents the residual function.

5. Conclusions and Future Scope

The data obtained from using AI in Breast Cancer Detection represents significant progress in accurately identifying and categorizing cancerous areas within MRI images. The model's performance metrics, such as loss, IOU (Intersection over Union), and F-Score, exhibit a consistent and positive trend throughout the training process. This trend indicates the model's ability to grasp essential features crucial for effectively detecting breast cancer-related regions.

Looking ahead, there are several avenues to further enhance this AI-driven approach. Firstly, researchers can delve into more intricate model architectures, exploring advanced techniques like attention mechanisms or transformer-based models. Integrating information from multiple sources and pre-trained models is utilized, can expedite training and enhance the model's ability to generalize to unseen data.

Furthermore, conducting extensive clinical validation studies using diverse datasets is imperative to verify the model's effectiveness and reliability and it's reliable and explainable in the real world By making the model's decision-making process transparent and understandable, it becomes more suitable for adoption in clinical practice.

Ultimately, these efforts aim to not only improve the accuracy and performance of the AI model but also ensure its practicality, reliability, and acceptance in the healthcare domain. This advancement in Breast Cancer Detection using AI holds the potential to contribute significantly to early diagnosis, personalized treatment strategies, and improved outcomes for breast cancer patients.

References

1. Rishav Singh, Tanveer Ahmed, Abhinav Kumar, Amit Kumar Singh, Anil Kumar Pandey, Sanjay Kumar Singh, "Imbalanced Breast Cancer Classification Using Transfer Learning," IEEE.

2. Kui Liu, Guixia Kang, Ningbo Zhang, Beibei Hou, "Breast Cancer Classification Based on Fully-Connected Layer First Convolutional Neural Networks," IEEE.

3. Nisreen I.R. Yassin, Shaimaa Omran, Enas M.F. El Houby, Hemat Allam, "Machine learning techniques for breast cancer computer aided diagnosis using different image modalities: A systematic review," Computer Methods and Programs in Biomedicine, vol. 156, pp. 25-45, March 2018, doi: 10.1016/j.cmpb.2017.10.019.

4. Naresh Khuriwal, Nidhi Mishra, "Breast Cancer Diagnosis Using Deep Learning Algorithm," IEEE Access, vol. 9.

5. Abeer Saber, Mohamed Sakr, Osama M. Abo-Seida, Arabi Keshk, Huiling Chen, "A Novel Deep-Learning Model for Automatic Detection and Classification of Breast Cancer Using the Transfer-Learning Technique," IEEE.

6. Dana Bazazeh, Raed Shubair, "Comparative study of machine learning algorithms for breast cancer detection and diagnosis," IEEE Systems Journal, vol. 8, issue 3.

7. Yasmeen Mourice George, Hala Helmy Zayed, Mohamed Ismail Roushdy, Bassant Mohamed Elbagoury, "Remote Computer-Aided Breast Cancer Detection and Diagnosis System Based on Cytological Images," IEEE.

8. Yasin Yari, Thuy V. Nguyen, Hieu T. Nguyen, "Deep Learning Applied for Histological Diagnosis of Breast Cancer," IEEE.

9. Narbada Prasad Gupta, Praveen Kumar Malik, Bhagwan Shree Ram, "A Review on Methods and Systems for Early Breast Cancer Detection," IEEE Access, vol. 7.

10. Zhiqiong Wang, Mo Li, Huaxia Wang, Hanyu Jiang, Yudong Yao, Hao Zhang, Junchang Xin, "Breast Cancer Detection Using Extreme Learning Machine Based on Feature Fusion With CNN Deep Features," IEEE Access, vol. 7.

RE-2022-269188-plag-report

ORIGINALITY REPORT

4%	1%	3%	1%
SIMILARITY INDEX	INTERNET SOURCES	PUBLICATIONS	STUDENT PAPERS

PRIMARY SOURCES

1	Monika Agarwal, Geeta Rani, Ambeshwar Kumar, Pradeep Kumar K, R. Manikandan, Amir H. Gandomi. "Deep Learning for Enhanced Brain Tumor Detection and Classification", Results in Engineering, 2024 Publication	1%
2	Submitted to The Robert Gordon University Student Paper	1%
3	www.e3s-conferences.org Internet Source	<1%
4	www.medrxiv.org Internet Source	<1%
5	dokumen.pub Internet Source	<1%
6	"Neural Information Processing", Springer Science and Business Media LLC, 2017 Publication	<1%
7	Khalil ur Rehman, Jianqiang Li, Yan Pei, Anaa Yasin, Saqib Ali, Yousaf Saeed. "Architectural Distortion-Based Digital Mammograms	<1%

Classification Using Depth Wise Convolutional Neural Network", Biology, 2021
Publication

8 Hosameldin O. A. Ahmed, Asoke K. Nandi. "Chapter 9 Colour Clustering and Deep Transfer Learning Techniques for Breast Cancer Detection Using Mammography Images", Springer Science and Business Media LLC, 2024 <1%
Publication

Exclude quotes	On	Exclude matches	Off
Exclude bibliography	On		

RE-2022-269188-plag-report

GRADEMARK REPORT

FINAL GRADE

/100

GENERAL COMMENTS

PAGE 1

PAGE 2

PAGE 3

PAGE 4

PAGE 5

PAGE 6

PAGE 7

PAGE 8

PAGE 9

PAGE 10

PAGE 11

PAGE 12

PAGE 13

PAGE 14